

Nuclear Physics from Lattice QCD*

Martin J. Savage^{†1}

¹Department of Physics, University of Washington,
Box 351560, Seattle, WA 98195, USA.

October 28, 2011

Abstract

I review recent progress in the development of Lattice QCD into a calculational tool for nuclear physics. Lattice QCD is currently the only known way of “solving” QCD in the low-energy regime, and it promises to provide a solid foundation for the structure and interactions of nuclei directly from QCD.

1 Introduction

As discovered by the New Zealand physicist Ernest Rutherford, a nucleus, labeled by its baryon number and electric charge, is at the heart of every atom. Loosely speaking, nuclei are collections of protons and neutrons that interact pairwise, with much smaller, but significant, three-body interactions. We are in the fortunate situation of knowing the underlying laws governing the strong interactions. It is the quantum field theory called quantum chromodynamics (QCD), constructed in terms of quark and gluon fields with interaction determined by a local SU(3) gauge-symmetry, along with quantum electrodynamics (QED), that underpins all of nuclear physics when the five relevant input parameters, the scale of strong interactions Λ_{QCD} , the three light-quark masses m_u , m_d and m_s , and the electromagnetic coupling α_e , are set to their values in nature. It is remarkable that the complexity of nuclei emerges from “simple” gauge theories with just five input parameters. Perhaps even more remarkable is that nuclei resemble collections of nucleons and not collections of quarks and gluons. By solving QCD, we will be able to predict, with arbitrary precision, nuclear processes and the properties of multi-baryon systems (including, for instance, the interior of neutron stars).

The fine-tunings observed in the structure of nuclei and the interactions between nucleons are peculiar and fascinating aspects of nuclear physics. For the values of the input parameters that we have in our universe, the nucleon-nucleon (NN) interactions are fine-tuned to produce unnaturally large scattering lengths in both s-wave channels (described by non-trivial fixed-points in the low-energy effective field theory (EFT)), and the energy levels in the ^8Be -system, ^{12}C and ^{16}O are in “just-so” locations to produce enough ^{12}C to support life, and the subsequent emergence and evolution of the human species.

*Lecture presented at the Erice School on Nuclear Physics 2011: *From Quarks and Gluons to Hadrons and Nuclei*, organized by A. Faessler and J. Wambach.

[†][NPLQCD Collaboration]

At a fundamental level it is important for us to determine the sensitivity of the abundance of ^{12}C to the light-quark masses and to ascertain the degree of their fine-tuning.

Being able to solve QCD for the lightest nuclei, using the numerical technique of Lattice QCD (LQCD), would allow for a partial unification of nuclear physics. It would be possible to “match” the traditional nuclear physics techniques - the solution of the quantum many-body problem for neutrons and protons using techniques such as No-Core Shell Model (NCSM), Greens function Monte Carlo (GFMC), and others, to make predictions for the structure and interactions of nuclei for larger systems than can be directly calculated with LQCD. By placing these calculations on a fundamental footing, reliable predictions with quantifiable uncertainties can then be made for larger systems.

2 Lattice QCD Calculations of Nuclear Correlation Functions

Lattice QCD is a technique in which space-time is discretized into a four-dimensional grid and the QCD path integral over the quark and gluon fields at each point in the grid is performed in Euclidean space-time using Monte Carlo methods. A LQCD calculation of a given quantity will deviate from its value in nature because of the finite volume of the space-time (with $L^3 \times T$ lattice points) over which the fields exist, and the finite separation between space-time points (the lattice spacing, b). However, such deviations can be systematically removed by performing calculations in multiple volumes with multiple lattice spacings, and extrapolating using the theoretically known functional dependences on each. Supercomputers are needed for such calculations due to the number of space-time points (sub grids of which are distributed among the compute cores) and the Monte Carlo evaluation of the path integral over the dynamical fields. In order for a controlled continuum extrapolation, the lattice spacing must be small enough to resolve structures induced by the strong dynamics, encapsulated by $b\Lambda_\chi \ll 1$ where Λ_χ is the scale of chiral symmetry breaking. Further, in order to have the hadron masses, and also the scattering observables, exponentially close to their infinite volume values, the lattice volume must be large enough to contain the lightest strongly interacting particle, encapsulated by $m_\pi L \gtrsim 2\pi$ where m_π is the mass of the pion and L is the extent of the spatial dimension of the cubic lattice volume (this, of course, can be generalized to non-cubic volumes). Effective field theory (EFT) descriptions of these observables exist for $b\Lambda_\chi \lesssim 1$ (the Symanzik action and its translation into χ PT and other frameworks) and $m_\pi L \gtrsim 2\pi$ (the p-regime of χ PT and other frameworks). The low-energy constants in the appropriate EFT are fit to the results of the LQCD calculations, which are then used to take the limit $b \rightarrow 0$ and $L \rightarrow \infty$. As the computational resources available today for LQCD calculations are not sufficient to be able to perform calculations at the physical values of the light quark masses in large enough volumes and at small enough lattice spacings, realistic present day calculations are performed at light quark masses that yield pion masses of $m_\pi \sim 200$ MeV. Therefore, present day calculations require the further extrapolation of $m_q \rightarrow m_q^{\text{phys}}$, but do not yet include strong isospin breaking or electromagnetism. In principle, the gluon field configurations that are generated in LQCD calculations can be used to calculate an enormous array of observables, spanning the range from particle to nuclear physics. In practice, this is becoming less common, largely due to the different scales relevant to particle physics and to nuclear physics. Calculations of quantities involving the pion with a mass of $m_\pi \sim 140$ MeV are substantially different from those of, say, the triton with a mass of $M(^3\text{H}) \sim 3$ GeV, and with the typical scale of nuclear excitations being $\Delta E \sim 1$ MeV. Present day dynamical LQCD calculations of nuclear physics quantities are performed with $m_\pi \sim 400$ MeV, lattice spacings of $b \sim 0.1$ fm and volumes with spatial extent of $L \sim 4$ fm. Quenched calculations, which unfortunately cannot be connected to nature, are typically performed in larger volumes as the gauge-field configurations are less expensive to generate compared with dynamical configurations.

LQCD calculations are approached in the same way that experimental efforts use detectors to measure one or more quantities - the computer is equivalent to the accelerator and the algorithms, software

stack, and parameters of the LQCD calculation(s) are the equivalent of the detector. The parameters, such as lattice spacing, quark masses and volume, are selected based upon available computational resources, and simulations of the precision of the calculation(s) required to impact the physical quantity of interest, i.e. simulations of the LQCD Monte Carlo's are performed. The size of the computational resources required for cutting edge calculations are such that you only get “one shot at it”. A typical work-flow of a LQCD calculation consists of three major components. The first component is the production of an ensemble of gauge-field configurations which contain statistically independent samplings of the gluon field configuration resulting from the LQCD action. The production of gauge-fields requires the largest partitions on the leadership class computational facilities, typically requiring $\gtrsim 128\text{K}$ compute cores. Present day calculations have $n_f = 0, 2, 2 + 1, 3, 2 + 1 + 1$ dynamical light quark flavors and use the Wilson, $\mathcal{O}(b)$ -improved-Wilson, staggered (Kogut-Susskind), domain-wall or overlap discretizations, each of which have their own “features”. It is the evaluation of the light-quark determinant (the determinant of a sparse matrix with dimensions $\gtrsim 10^8 \times 10^8$) that consumes the largest fraction of the resources. Roughly speaking, $\gtrsim 10^4$ HMC trajectories are required to produce an ensemble of 10^3 decorrelated gauge-fields, but in many instances this is an under-estimate. For observables involving quarks, a second component of production is the determination of the light-quark propagators on each of the configurations. The light-quark propagator from a given source point is determined by an iterative inversion of the quark two-point function, using the conjugate-gradient (CG) algorithm or variants thereof such as BiCGSTAB, an example of which is shown in Figure 1. During the last couple of years,

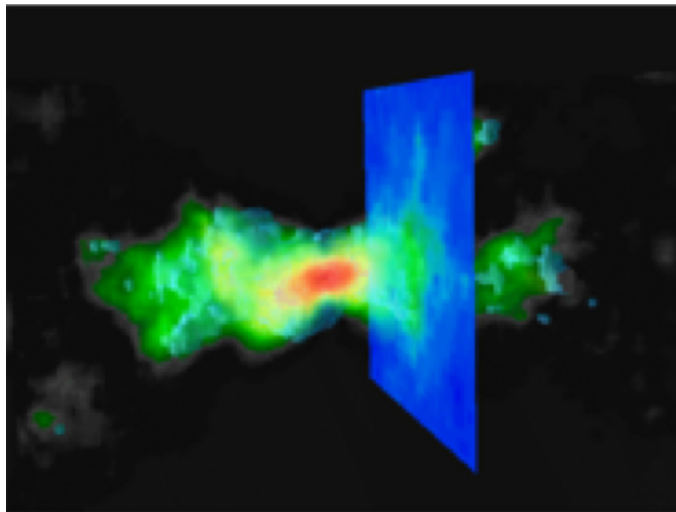


Figure 1: An example of (the real part of one component of) a light-quark propagator. The (blue) “wall” corresponds to the anti-periodic boundary conditions imposed in the time direction. [Image is reproduced with the permission of R. Gupta.]

the propagator production codes have been ported to run on GPU machines in parallel. The GPU's can perform propagator calculations faster than standard CPU's by one or two orders of magnitude, and have led to a major reduction in the statistical uncertainties in many calculations. There have been numerous algorithm developments that have also reduced the resources required for propagator production, such as the implementation of deflation techniques and the use of multi-grid methods. The third component of a LQCD calculation is the production of correlation functions from the light-quark propagators. This involves performing all of the Wick contractions that contribute to a given quantity. The number of contractions required for computing a single hadron correlation function is small. However, to acquire long plateaus in the effective mass plots (EMP's) that persist to short times, Lüscher-Wolff type methods [1, 2] involve the computation of a large number of correlation functions resulting from

different interpolating operators, and the number of contractions can become large. In contrast, the naive number of contractions required for a nucleus quickly becomes astronomically large ($\sim 10^{1500}$ for uranium), but symmetries in the contractions greatly reduces this number. For instance, there are 2880 naive contractions contributing to the ${}^3\text{He}$ correlation function, but only 93 are independent. As a light-quark propagator can give rise to a pion correlation function ($\sim e^{-m_\pi t}$) and a nucleon correlation function ($\sim e^{-m_N t}$) (and many other hadronic correlation functions), it is clear that the propagator contains a hierarchy of mass scales, and that significant cancellations between various components of the propagator occur in nucleon (and hence nuclear) correlation functions. When taking a high power of the propagator, rounding errors can accumulate, and in some cases it becomes necessary to perform calculations using “arbitrary precision” libraries - for instance `apprec`. A further consequence of the hierarchy of mass scales is that there is an asymptotic signal-to-noise problem in nuclear correlation functions. The ratio of the mean value of the correlation function to the variance of the sample from which the mean is evaluated degrades exponentially at large times. However, this is absent at short and intermediate times and the exponential degradation of the signal-to-noise in the correlation functions can be avoided.

3 Lattice QCD Calculations of Multi-Hadron Systems

A driver for the development of LQCD technology is the reproduction of the high-precision, experimentally determined, nucleon-nucleon phase-shift data (verifying the LQCD technology) and the subsequent predictions of comparable precision for hyperon-nucleon (YN), hyperon-hyperon (YY) interactions, along with three-baryon (including nnn) and higher-body interactions. When completed, the precision of these latter observables will greatly exceed what is possible experimentally, and therefore refine our ability to calculate the properties exotic states of matter such as hyper-nuclei and the interior of neutron stars, and to reduce the uncertainty in the fusion cross section of light nuclei. Unfortunately, the formalism that is currently in place that allows for the use of LQCD to extract information impacting phenomenology is somewhat limited. In fact, beyond the direct calculation of binding energies, it is presently limited to using Lüscher’s method to determine the scattering amplitude below inelastic thresholds in $2 \rightarrow 2$ processes ¹, with straightforward extensions to coupled channels systems.

3.1 Euclidean Space Correlation Functions

Most Euclidean space correlation functions computed in LQCD calculations (suitably Fourier transformed) are the sums of exponential functions. The arguments of the exponentials are the product of Euclidean time with the eigenvalues of the Hamiltonian associated with eigenstates in the finite-volume that couple to the hadronic sources and sinks. For a lattice that has infinite extent in the time-direction, the correlation function at large times becomes a single exponential dictated by the ground state energy and the overlap of the source and sink with the ground state. As an example, consider the pion two-point function, $C_{\pi^+}(t)$, generated by a source (and sink) of the form $\pi^+(\mathbf{x}, t) = \bar{u}(\mathbf{x}, t)\gamma_5 d(\mathbf{x}, t)$,

$$C_{\pi^+}(t) = \sum_{\mathbf{x}} \langle 0 | \pi^-(\mathbf{x}, t) \pi^+(\mathbf{0}, 0) | 0 \rangle \quad , \quad (1)$$

where the sum over all lattice sites at each time-slice, t , projects onto the $\mathbf{p} = \mathbf{0}$ spatial momentum states. The source $\pi^+(\mathbf{x}, t)$ not only produces single pion states, but also all states with the quantum

¹ While it has been suggested that one can extract nuclear “potentials” from LQCD calculations, these energy-dependent and lattice scheme dependent quantities contain no more information than the energy-eigenvalues (and hence the scattering phase shift determined at the energy-eigenvalues via Lüscher’s method). It is important to recognize the fact that these “potentials” produce scheme-dependent values of the scattering amplitude at energies away from the energy-eigenvalues. As such, when used, for instance, in a nuclear many-body calculation, they will produce results that are not predictions of QCD.

numbers of the pion. More generally, the source and sink are smeared over lattice sites in the vicinity of (\mathbf{x}, t) to increase the overlap onto the ground state and lowest-lying excited states. Translating the sink operator in time via $\pi^+(\mathbf{x}, t) = e^{\hat{H}t}\pi^+(\mathbf{x}, 0)e^{-\hat{H}t}$, and inserting a complete set of states, gives ²

$$C_{\pi^+}(t) = \sum_n \frac{e^{-E_n t}}{2E_n} \sum_{\mathbf{x}} \langle 0 | \pi^-(\mathbf{x}, 0) | n \rangle \langle n | \pi^+(\mathbf{0}, 0) | 0 \rangle \rightarrow A_0 \frac{e^{-m_\pi t}}{2m_\pi} . \quad (2)$$

At finite lattice spacing, the correlation functions for Wilson fermions remain sums of exponential functions, but for particular choices of parameters used in the domain-wall discretization, the correlation functions exhibit additional sinusoidally modulated exponential behavior at short-times with a period set by the lattice spacing [3]. It is straightforward to show that the lowest energy eigenvalue extracted from the correlation function in Eqs. (1) and (2) corresponds to the mass of the π^+ (and, more generally, the mass of the lightest hadronic state that couples to the source and sink) in the finite volume. The masses of stable single particle states can be extracted from a Lattice QCD calculation with high accuracy as long as the lattice spatial extent is large compared to the pion Compton-wavelength ³.

3.2 Hadronic Interactions, the Maiani-Testa Theorem and Lüscher's Method

Extracting hadronic interactions from Lattice QCD calculations is more complicated than the determination of the spectrum of stable particles. This is encapsulated in the Maiani-Testa theorem [5], which states that S-matrix elements cannot be extracted from infinite-volume Euclidean-space Green functions except at kinematic thresholds. This could be problematic from the nuclear physics perspective, as a main motivation for pursuing Lattice QCD is to compute nuclear reactions involving multiple nucleons. Of course, it is clear from the statement of this theorem how it can be evaded, Euclidean-space correlation functions are calculated at finite volume to extract S-matrix elements, the formulation of which was known for decades in the context of non-relativistic quantum mechanics [6] and extended to quantum field theory by Lüscher [7, 8]. The energy of two particles in a finite volume depends in a calculable way upon their elastic scattering amplitude and their masses for energies below the inelastic threshold. As a concrete example consider $\pi^+\pi^+$ scattering. A $\pi^+\pi^+$ correlation function in the A_1^+ representation of the cubic group [9] (that projects onto the continuum s-wave state amongst others) is

$$C_{\pi^+\pi^+}(p, t) = \sum_{|\mathbf{p}|=p} \sum_{\mathbf{x}, \mathbf{y}} e^{i\mathbf{p}\cdot(\mathbf{x}-\mathbf{y})} \langle \pi^-(t, \mathbf{x}) \pi^-(t, \mathbf{y}) \pi^+(0, \mathbf{0}) \pi^+(0, \mathbf{0}) \rangle . \quad (3)$$

In relatively large lattice volumes, the energy difference between the interacting and non-interacting two-meson states is a small fraction of the total energy, which is dominated by the masses of the mesons. This energy difference can be extracted from the ratio of correlation functions, $G_{\pi^+\pi^+}(p, t)$, where

$$G_{\pi^+\pi^+}(p, t) \equiv \frac{C_{\pi^+\pi^+}(p, t)}{C_{\pi^+}(t)C_{\pi^+}(t)} \rightarrow \mathcal{B}_0 e^{-\Delta E_0 t} , \quad (4)$$

and where the arrow denotes the large-time behavior of $G_{\pi^+\pi^+}$. For calculations performed with $p = 0$, the energy eigenvalue, E_n , and its deviation from the sum of the rest masses of the particle, ΔE_n , are related to a momentum magnitude p_n by

$$\Delta E_n \equiv E_n - 2m_\pi = 2\sqrt{p_n^2 + m_\pi^2} - 2m_\pi . \quad (5)$$

To obtain $k \cot \delta(k)$, where $\delta(k)$ is the phase shift, the square of p_n is extracted from the energy shift and inserted into [6, 7, 8, 10]

$$k \cot \delta(k) = \frac{1}{\pi L} \mathbf{S} \left(\left(\frac{kL}{2\pi} \right)^2 \right) , \quad \mathbf{S}(x) \equiv \sum_{|\mathbf{j}| < \Lambda} \frac{1}{|\mathbf{j}|^2 - x} - 4\pi\Lambda , \quad (6)$$

²The absence of external electroweak fields that may exert forces on hadrons in the lattice volume is assumed.

³Finite-volume effects are exponentially suppressed [4] by factors of $e^{-m_\pi L}$ in large volumes.

where $k = p_n$, and which is only valid below the inelastic threshold. The regulated three-dimensional sum [11] extends over all triplets of integers \mathbf{j} such that $|\mathbf{j}| < \Lambda$ and the limit $\Lambda \rightarrow \infty$ is implicit. Therefore, by calculating the energy-shift, ΔE_n , of the two particles in the finite lattice volume, the scattering phase-shift is determined at ΔE_n . In the absence of interactions between the particles, the energy eigenstates in the finite volume occur at momenta $\mathbf{p} = 2\pi\mathbf{j}/L$. Perhaps most important for nuclear physics is that this expression is valid for large and even infinite scattering lengths [11]. The only restriction is that the lattice volume be much larger than the range of the interaction between the hadrons, which for two nucleons, is set by the mass of the pion.

3.3 Meson-Meson Scattering

The low-energy scattering of pions and kaons, the pseudo-Goldstone bosons of spontaneous chiral symmetry breaking, provides a perfect testing ground for Lattice QCD calculations of scattering parameters. There is little or no signal-to-noise problem in such calculations and therefore highly accurate Lattice QCD calculations of stretched-isospin states can be performed with modest computational resources. Moreover, the EFTs which describe the low-energy interactions of pions and kaons, including lattice-spacing and finite-volume effects, have been developed to non-trivial orders in the chiral expansion. The

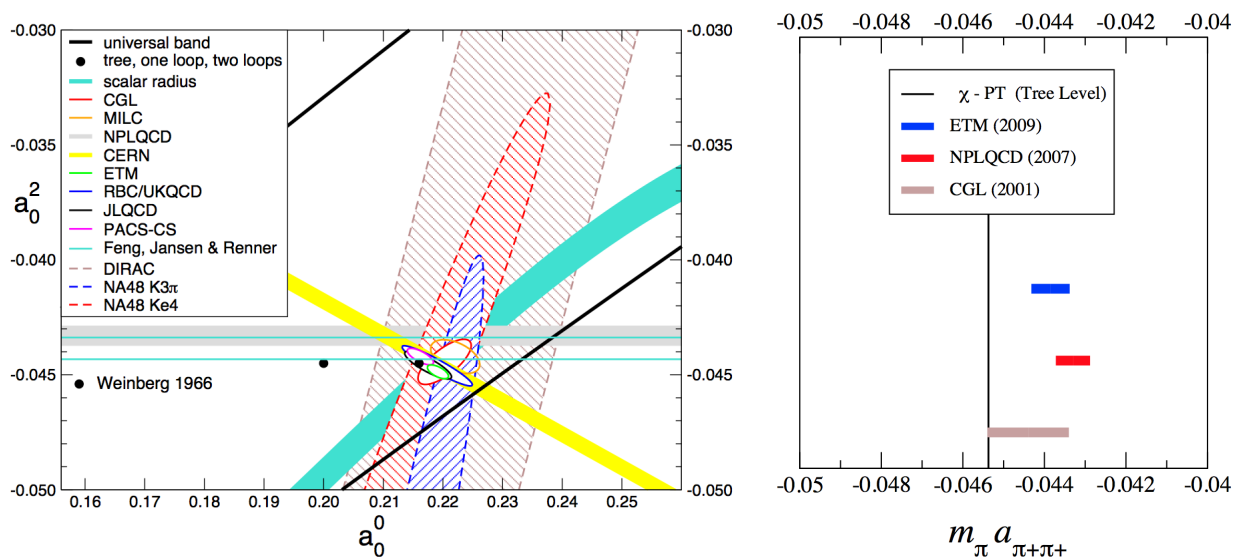


Figure 2: Present constraints on threshold s-wave $\pi\pi$ scattering. Noteworthy in the left panel [14] are the red ellipse from the Roy equation analysis and the grey band from the direct Lattice QCD calculation of the $\pi^+\pi^+$ scattering length, as discussed in the text. The right panel shows the $\pi^+\pi^+$ scattering length results only. [Image in the left panel is reproduced with the permission of H. Leutwyler.]

$I = 2$ pion-pion ($\pi^+\pi^+$) scattering length serves as a benchmark calculation with an accuracy that can only be aspired to in other systems. The scattering lengths for $\pi\pi$ scattering in the s-wave are uniquely predicted at LO in χ -PT [12]:

$$m_{\pi^+} a_{\pi\pi}^{I=0} = 0.1588 \quad , \quad m_{\pi^+} a_{\pi\pi}^{I=2} = -0.04537 \quad . \quad (7)$$

While experiments do not directly provide stringent constraints on the scattering lengths, a determination of s-wave $\pi\pi$ scattering lengths using the Roy equations has reached a remarkable level of precision [13, 14]:

$$m_{\pi^+} a_{\pi\pi}^{I=0} = 0.220 \pm 0.005 \quad , \quad m_{\pi^+} a_{\pi\pi}^{I=2} = -0.0444 \pm 0.0010 \quad . \quad (8)$$

The Roy equations [15] use dispersion theory to relate scattering data at high energies to the scattering amplitude near threshold. At present, Lattice QCD can compute $\pi\pi$ scattering only in the $I = 2$ channel with precision as the $I = 0$ channel contains disconnected diagrams which require large computational resources. It is of great interest to compare the precise Roy equation predictions with Lattice QCD calculations, and Figure 2 summarizes theoretical and experimental constraints on the s-wave $\pi\pi$ scattering lengths [14]. This is clearly a strong-interaction process for which theory has somewhat out-paced the challenging experimental measurements.

Mixed-action $n_f = 2 + 1$ Lattice QCD calculations, employing domain-wall valence quarks on a rooted staggered sea and combined with mixed-action χ PT, have predicted [16]

$$m_{\pi^+} a_{\pi\pi}^{I=2} = -0.04330 \pm 0.00042 \quad , \quad (9)$$

at the physical pion mass, where the statistical and systematic uncertainties have been combined in quadrature. The agreement between this result and the Roy equation determination is a striking confirmation of the lattice methodology, and a powerful demonstration of the constraining power of chiral symmetry in the meson sector. However, lattice calculations at one or more smaller lattice spacings, and with different discretizations, are required to verify and further refine this calculation. The ETM collaboration has performed a $n_f = 2$ calculation of the $I = 2$ $\pi\pi$ scattering length [17], producing a result extrapolated to the physical pion mass of

$$m_{\pi^+} a_{\pi\pi}^{I=2} = -0.04385 \pm 0.00028 \pm 0.00038 \quad . \quad (10)$$

It is interesting to compare the pion mass dependence of the meson-meson scattering lengths to the current algebra predictions. In Figure 3 (left panel) one sees that the $I = 2$ $\pi\pi$ scattering length is consistent with the current algebra result up to pion masses that are expected to be at the edge of the chiral regime in the two-flavor sector. While in the two flavor theory one expects fairly good convergence of the chiral expansion and, moreover, one expects that the effective expansion parameter is small in the channel with maximal isospin, the lattice calculations clearly imply a degree of cancellation between chiral logs and counterterms. However, as one sees in Figure 3 (right panel), the same phenomenon occurs in K^+K^+ where the chiral expansion is governed by the strange quark mass and is therefore expected to be much more slowly converging. This remarkable conspiracy between chiral logs and counterterms for the meson-meson scattering lengths remains mysterious.

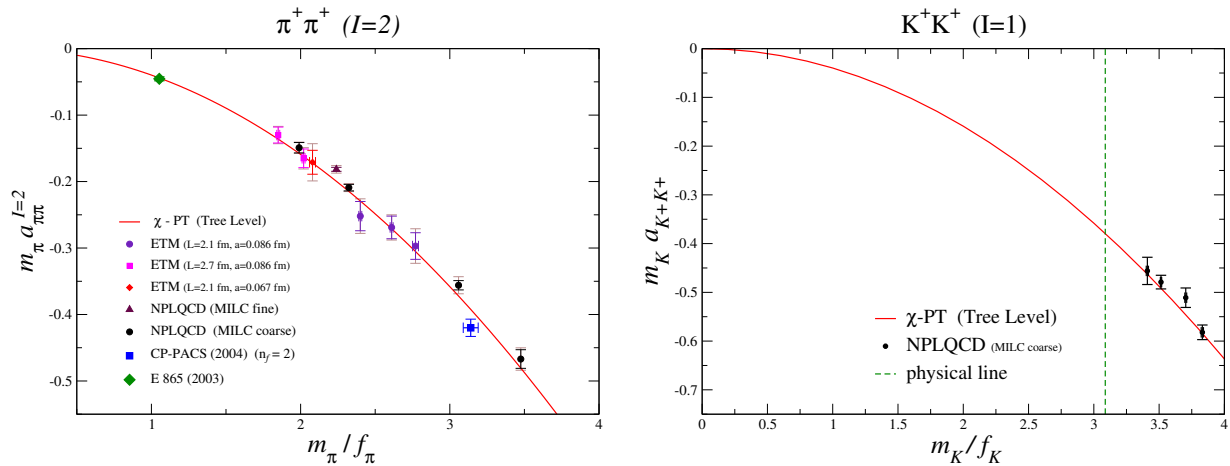


Figure 3: $m_{\pi^+} a_{\pi^+\pi^+}$ vs. m_{π^+}/f_{π^+} (left panel) and $m_{K^+} a_{K^+K^+}$ vs. m_{K^+}/f_{K^+} (right panel). The solid (red) curves are the current algebra predictions.

LQCD calculations of the meson-meson scattering phase-shifts are much less advanced than of the scattering length. This is because the calculation of the phase shift, $\delta(E)$, at a given energy, E , requires a lattice calculation of the two-meson correlation function at the energy E . Generally speaking, a given calculation can determine the lowest few two-hadron energy eigenvalues for a given momentum of the center-of-mass, and that multiple lattice volumes will allow for additional values of E at which to determine $\delta(E)$. The first serious calculation of the s-wave ($l = 0$) $I = 2$ $\pi\pi$ phase-shift was done by the CP-PACS collaboration with $n_f = 2$ at a relatively large pion mass [18], and recently two groups have performed calculations at lower pion masses [19, 20], the results of which are shown in Figure 4. Further, in some nice work by the Hadron Spectrum Collaboration (HSC), the first efforts have been

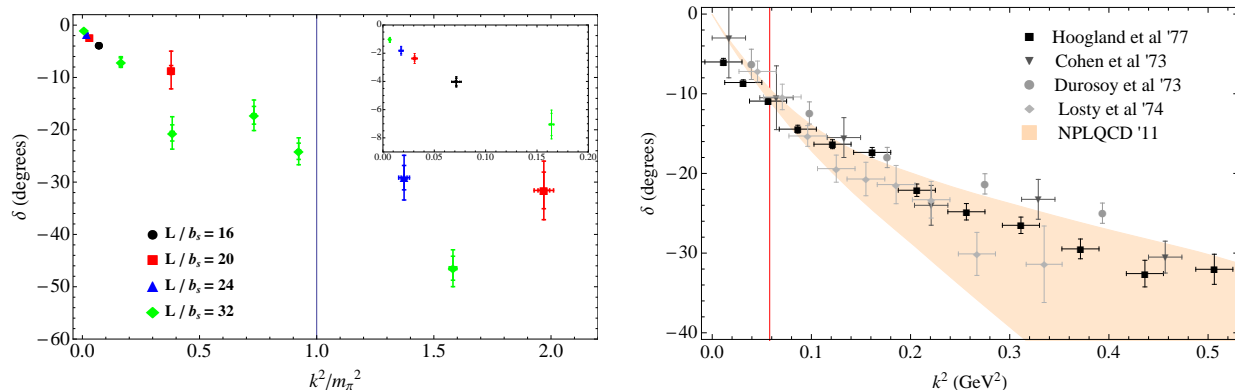


Figure 4: The $\pi^+\pi^+$ scattering phase-shift. The left panel shows the results of the LQCD calculations below the inelastic threshold ($|\mathbf{k}|^2 = 3m_\pi^2$) at a pion mass of $m_\pi \sim 390$ MeV [20], obtained on anisotropic Clover gauge-field configurations with a spatial lattice spacing of $b \sim 0.123$ fm, an anisotropy of $\xi \sim 3.5$ and spatial extents of $L = 16b, 20b, 24b$ and $32b$. The vertical (blue) line denotes the start of the t-channel cut. The shaded region in the right panel shows the results of the LQCD calculation extrapolated to the physical pion mass using NLO χ PT, while the points and uncertainties corresponds to the existing experimental data. The vertical (red) line corresponds to the inelastic threshold.

made to extract the d-wave ($l = 2$) $I = 2$ $\pi\pi$ phase shift [19].

3.4 Two-Body Bound States

In nature, two nucleons in the ${}^3S_1 - {}^3D_1$ coupled channels bind to form the simplest nucleus (beyond the proton), the deuteron ($J^\pi = 1^+$), with a binding energy of $B_d = 2.224644(34)$ MeV, and nearly bind into a di-neutron in the 1S_0 channel. However, little is known experimentally about possible bound states in more exotic channels, for instance those containing strange quarks. The most famous exotic channel that has been postulated to support a bound state (the H-dibaryon [21]) has the quantum numbers of $\Lambda\Lambda$ (total angular momentum $J^\pi = 0^+$, isospin $I = 0$ and strangeness $s = -2$). In this channel, all six quarks in naive quark models, like the MIT bag model, can be in the lowest-energy single-particle state. Additionally, more extensive analyses using one-boson-exchange (OBE) models [22] and low-energy effective field theories (EFT) [23, 24], both constrained by experimentally measured nucleon-nucleon (NN) and hyperon-nucleon (YN) cross-sections and the approximate SU(3) flavor symmetry of the strong interactions, suggest that other exotic channels also support bound states. In the limit of SU(3) flavor symmetry, the 1S_0 -channels are in symmetric irreducible representations of $\mathbf{8} \otimes \mathbf{8} = \mathbf{27} \oplus \mathbf{10} \oplus \overline{\mathbf{10}} \oplus \mathbf{8} \oplus \mathbf{8} \oplus \mathbf{1}$, and hence the $\Xi^-\Xi^-$, $\Sigma^-\Sigma^-$, and nn (along with $n\Sigma^-$ and $\Sigma^-\Xi^-$) are in the $\mathbf{27}$. YN and NN scattering data, along with the leading SU(3) breaking effects from the

light-meson and baryon masses, suggest that $\Xi^-\Xi^-$ and $\Sigma^-\Sigma^-$ are bound at the physical values of the light-quark masses [22, 23, 24].

Recently, $n_f = 2 + 1$ calculations [25, 26], and subsequent $n_f = 3$ calculations [27], have provided evidence that the H-dibaryon is bound at a pion mass of $m_\pi \sim 390$ MeV [NPLQCD] and $m_\pi \sim 837$ MeV [HALQCD]⁴. The infinite-volume extrapolated H-dibaryon binding energy at $m_\pi \sim 390$ MeV is found to be

$$B_H^{(L=\infty)} = 13.2 \pm 1.8 \pm 4.0 \text{ MeV} \quad . \quad (11)$$

Possible extrapolations to the physical light-quark masses are shown in Figure 5, and suggest a weakly bound H-dibaryon or a near threshold resonance exists in this channel [28, 29, 30].

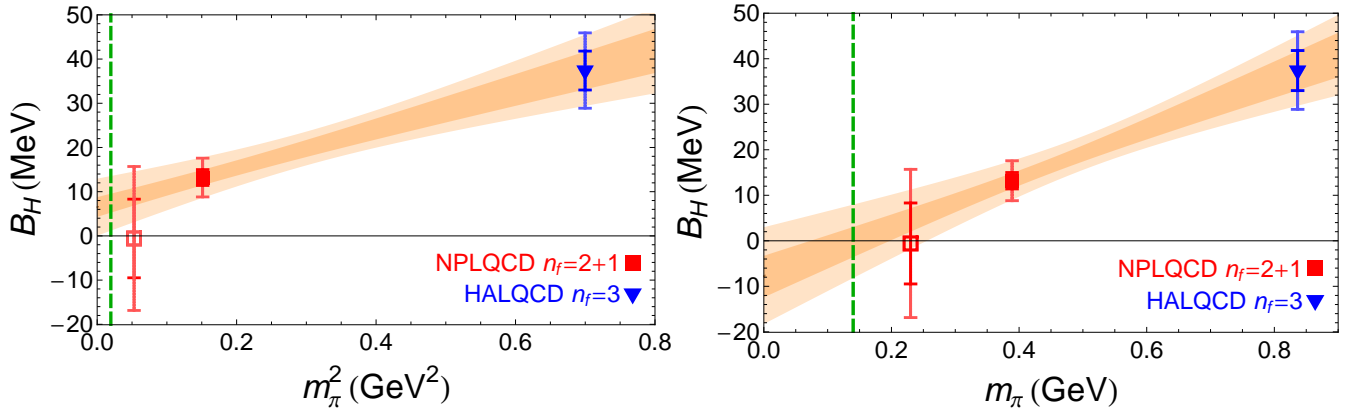


Figure 5: Possible extrapolations of the LQCD results for the binding of the H-dibaryon. The left panel corresponds to an extrapolation that is quadratic in m_π , of the form $B_H(m_\pi) = B_0 + d_1 m_\pi^2$, while the right panel corresponds to an extrapolation of the form $B_H(m_\pi) = \tilde{B}_0 + \tilde{d}_1 m_\pi$. In each panel, the red points are the result from the $n_f = 2 + 1$ calculations of NPLQCD [25, 26] while the blue point is from the $n_f = 3$ calculation of HALQCD [27]. The green dashed vertical line corresponds to the physical pion mass.

The NPLQCD collaboration has also found evidence that the $\Xi^-\Xi^-$ -system is bound at a pion mass of $m_\pi \sim 390$ MeV [26], as shown in Figure 6. This result, and the predictions of OBE models and leading order (LO) EFT, are shown in Figure 6. It is important to note that the uncertainty of the LQCD result is comparable to that of the OBE models and EFT results, and demonstrates that LQCD is approaching the time where it will provide more precise constraints on exotic systems than currently possible in the laboratory. It will be interesting to see whether J-PARC [31] or FAIR [32] can provide constraints on the $s = -3$ and $s = -4$ systems, as well as on the H-dibaryon [33]. The calculated binding energy of

$$B_{\Xi^-\Xi^-}^{(L=\infty)} = 14.0 \pm 1.4 \pm 6.7 \text{ MeV} \quad , \quad (12)$$

at $m_\pi \sim 390$ MeV provides strong motivation to return to OBE models and EFT frameworks and determine the expected dependence on the light-quark masses. The same LQCD calculations also found hints that both the deuteron and the di-neutron are bound at this same pion mass, with binding energies of

$$B_d^{(L=\infty)} = 11 \pm 5 \pm 12 \text{ MeV} \quad , \quad B_{nn}^{(L=\infty)} = 7.1 \pm 5.2 \pm 7.3 \text{ MeV} \quad . \quad (13)$$

The results of these calculations, along with the results of recent quenched calculations [34] are shown

⁴Both calculations were performed at approximately the same spatial lattice spacing of $b \sim 0.12$ fm.

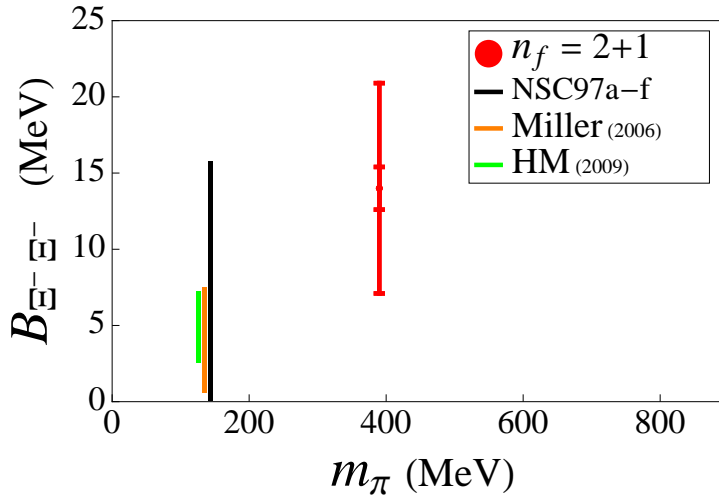


Figure 6: The $\Xi^- \Xi^-$ binding energy as a function of the pion mass. The black line denotes the predictions of the NSC97a-NSC97f models [22] constrained by nucleon-nucleon and hyperon-nucleon scattering data. The orange line denotes the range of predictions by Miller [23], and the green line denotes the leading order EFT prediction by Haidenbauer and Meissner (HM) [24]. The red point and uncertainty (the inner is statistical and the outer is statistical and systematic combined in quadrature) is the NPLQCD $n_f = 2 + 1$ result [26]. The OBE model and EFT predictions at the physical pion mass are displaced horizontally for the purpose of display.

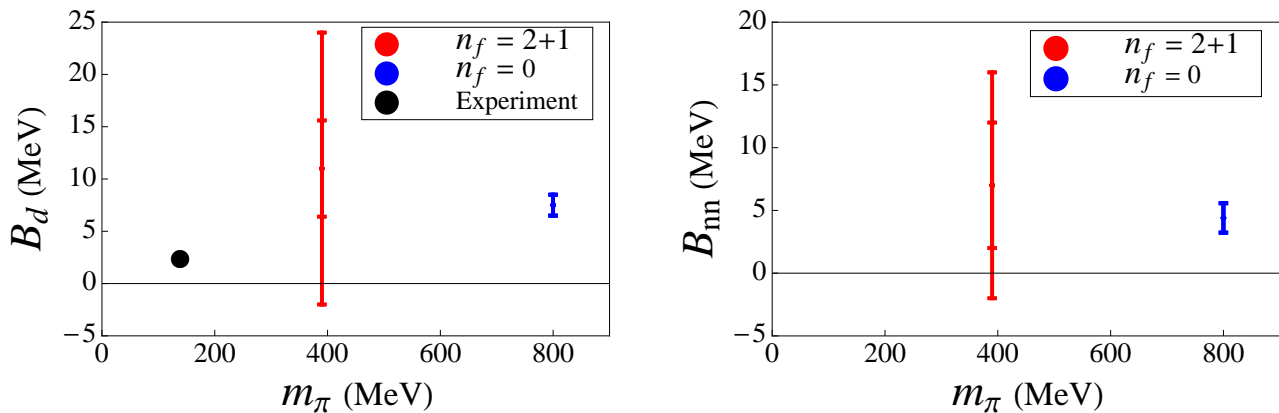


Figure 7: The deuteron (left panel) and di-neutron (right panel) binding energies as a function of the pion mass. The black circle denotes the experimental value. The blue points and uncertainties are from the quenched calculations of Ref. [34], while the red points and uncertainties (the inner is statistical and the outer is statistical and systematic combined in quadrature) are from the NPLQCD $n_f = 2 + 1$ calculations [26].

in Figure 7.

In late 2009, the PACS-CS collaboration performed the first quenched calculation of a four-baryon correlation function [35] in the α -particle (${}^4\text{He}$ nucleus) channel. The pion mass was $m_\pi \sim 800$ MeV and sea quark effects were ignored, however, this is a very important step towards calculating the properties and interactions of nuclei. Their results are shown in Figure 8, along with their result in the triton

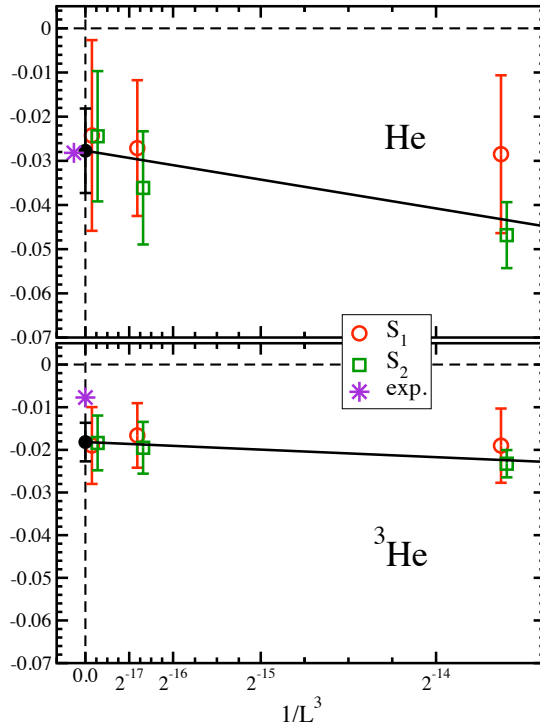


Figure 8: Quenched results for the binding energies (in lattice units) in the triton channel (lower panel) and the α -particle channel (upper panel) obtained by the PACS-CS collaboration [35]. The pion mass is $m_\pi \sim 800$ MeV. [Image is reproduced with the permission of the PACS-CS collaboration.]

channel, and significantly improved statistics are hoped for in the near future.

3.5 Nucleon-Nucleon Interactions

Perhaps the most studied and best understood of the two-hadron processes are proton-proton and proton-neutron scattering. In the s-wave, only two combinations of spin and isospin are possible, the spin-triplet isosinglet np (3S_1) and the spin-singlet isotriplet pp (1S_0), np (1S_0) and nn (1S_0). At the physical pion mass, the scattering lengths in these channels are unnaturally large and the ${}^3S_1 - {}^3D_1$ coupled-channel contains the deuteron. These large scattering lengths and the deuteron are described in EFT, by the coefficient of the momentum-independent four-nucleon operator being near a non-trivial fixed-point [36, 37] in its renormalization group flow at the physical light-quark masses. An interesting line of investigation is the study of the scattering lengths as a function of the quark masses to ascertain the sensitivity of this fine-tuning to the QCD parameters [38, 39, 40]. While the fine tuning is not expected to persist away from the physical masses, it is interesting to determine how the structure of nuclei depend upon the fundamental constants of nature.

The first study of baryon-baryon scattering with LQCD was performed more than a decade ago by Fukugita *et al* [41, 42]. Those calculations were quenched and at relatively large pion masses, $m_\pi \gtrsim 550$ MeV. Since that time, the dependence of the NN scattering lengths upon the light-quark masses has been determined to various non-trivial orders in the EFT expansion [38, 39, 40], which are estimated to be valid up to $m_\pi \sim 350$ MeV. Therefore, predictions of NN scattering parameters becomes possible with LQCD calculations that are performed with $m_\pi \lesssim 350$ MeV.

The NPLQCD collaboration performed the first $n_f = 2 + 1$ LQCD calculations of nucleon-nucleon

interactions [43] and hyperon-nucleon [44] interactions at low-energies but with unphysical pion masses, and the nucleon-nucleon scattering lengths were found to be of natural size. The fine-tunings at the physical values of the light-quark masses indicate that LQCD calculations with quark masses much closer to the physical values (than today) are needed to extrapolate to the experimental values. The results of the LQCD calculation at the lightest pion mass and the experimentally-determined scattering lengths at the physical value of the pion mass were used to constrain the chiral dependence of the scattering lengths from $m_\pi \sim 350$ MeV down to the chiral limit [43]. However, these results suggest various possible scenarios toward the chiral limit which can only be resolved by way of LQCD calculations at lighter pion masses. Summaries of existing LQCD calculations of the NN scattering lengths are shown in Figure 9. In contrast, very little is known about the interactions between nucleons and hyperons from experiment, and future LQCD calculations will likely provide the best determinations of the corresponding scattering parameters and hence determine the role of hyperons in neutron stars.

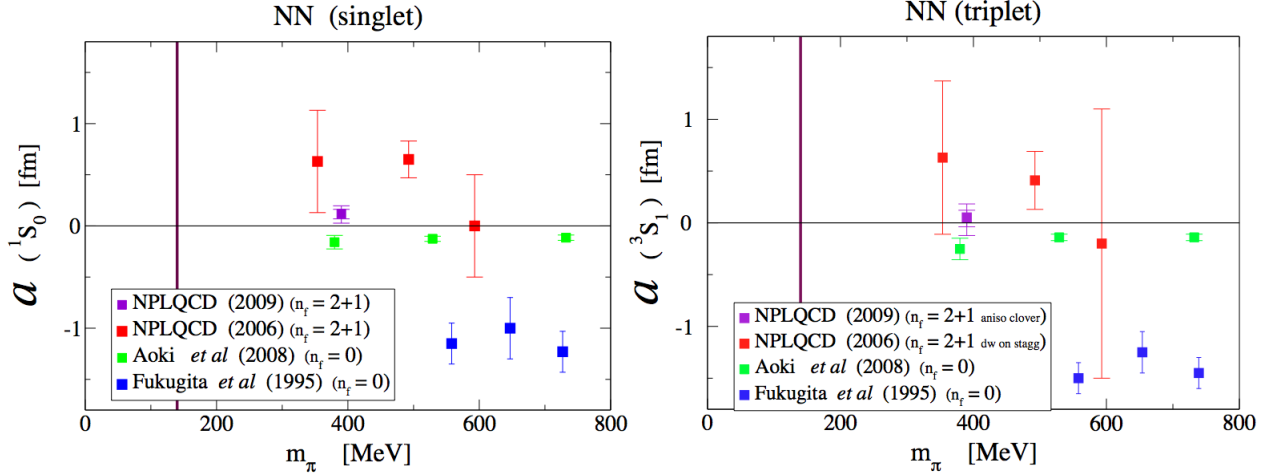


Figure 9: A compilation of the scattering lengths for NN scattering in the 1S_0 channel (left panel) and 3S_1 channel (right panel) calculated with LQCD [43, 45] and with quenched LQCD [46, 47, 48]. The vertical lines correspond to the physical pion mass.

3.6 Meson Condensates

The ground state of a generic system of many bosons with weak repulsive interactions is a Bose-condensate. A QCD system of pions and/or kaons form a Bose-Einstein condensate with fixed third-component of isospin, I_z , and strangeness, s , and it is of significant theoretical and phenomenological interest to investigate the properties of such systems. Theoretical efforts have used LO χ -PT to investigate the phase diagram at low chemical potential [49] and it is important to assess the extent to which these results agree with QCD, because in neutron stars, it is possible that it is energetically favorable to (partially-) electrically neutralize the system with a condensate of K^- mesons instead of electrons. Numerical calculations provide a probe of the dependence of the energy on the pion or kaon density, and thereby allow for an extraction of the chemical potential via a finite difference [50]. Results from mixed-action calculations of kaon condensates are shown in Figure 10 [50], along with the predictions of tree-level χ -PT, which are in remarkably good agreement. This is encouraging for studies of kaon condensation in neutron stars where, typically, tree level χ -PT interactions amongst kaons, and between kaons and baryons [51], are assumed. These calculations have been extended to mixed kaon-pion systems in Ref. [52].

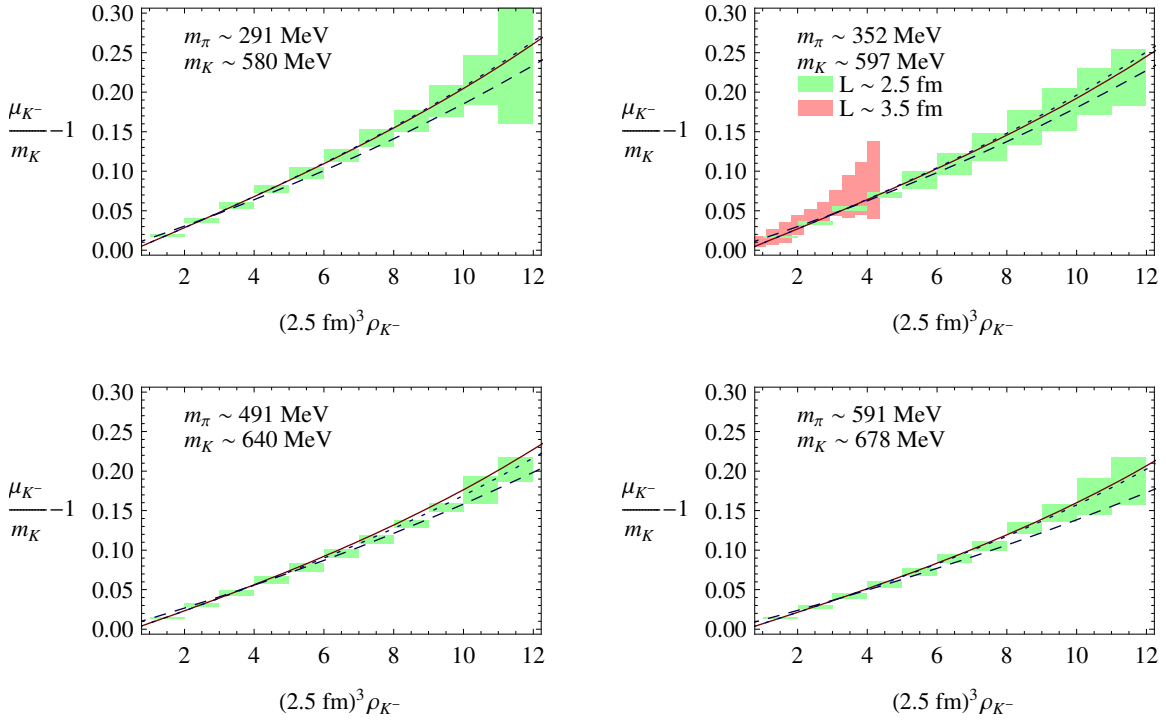


Figure 10: The dependence of the strangeness chemical potential on the kaon density [50]. The curves correspond to the predictions of tree level chiral perturbation theory (dashed) [49], the fitted energy shift (solid) and without the three-body interaction (dotted).

4 The Next Decade - the Drive Toward the Exa-scale

A number of workshops focusing on the science need for exa-scale computing resources sponsored by the US Department of Energy were held during 2009. One of the workshops, *Forefront Questions in Nuclear Science and the Role of Computing at the Extreme Scale* [53], established the need for exa-scale computing resources in order for the main goals of the field of nuclear physics to be accomplished [54]. One of the major goals of the field that requires exa-scale computing resources is the calculation of nuclear forces from QCD using Lattice QCD, and Figure 11 presents an overview of current estimates of these requirements.

As reviewed in Refs. [55, 56], a complete calculation of the nucleon-nucleon scattering amplitude, and the hyperon-nucleon and hyperon-hyperon scattering amplitudes (including multiple lattice spacings, volumes and light quark masses) will require sustained peta-scale resources, as shown in Figure 11. The same is true for the meson-baryon interactions. It is estimated that sustained sub-peta-flop-year resources are required to perform high-precision calculations of meson-meson scattering-phase shifts, including the contributions from disconnected diagrams to the isosinglet $\pi\pi$ channel. Further, it is estimated that sustained peta-scale resources are required in order to calculate the matrix elements of electroweak operators, such as those determining neutrino-induced breakup of the deuteron, in the few-nucleon sector. Significant progress is being made in computing single hadron matrix elements of such operators, such as the isovector axial-current matrix element in the nucleon, g_A [57, 58, 59]. While the extrapolation to the physical pion mass, and to infinite volume remain the subject of discussions in the community, relatively rapid progress is being made. Calculations of matrix elements of operators that receive contributions from disconnected diagrams remain difficult with currently available resources, but will be addressed with peta-scale resources. A significant uncertainty in the experimentally determined properties of neutrinos comes from the uncertainties in weak matrix elements between nuclear states. Such uncertainties in few-nucleon systems should be reduced within the next decade with anticipated

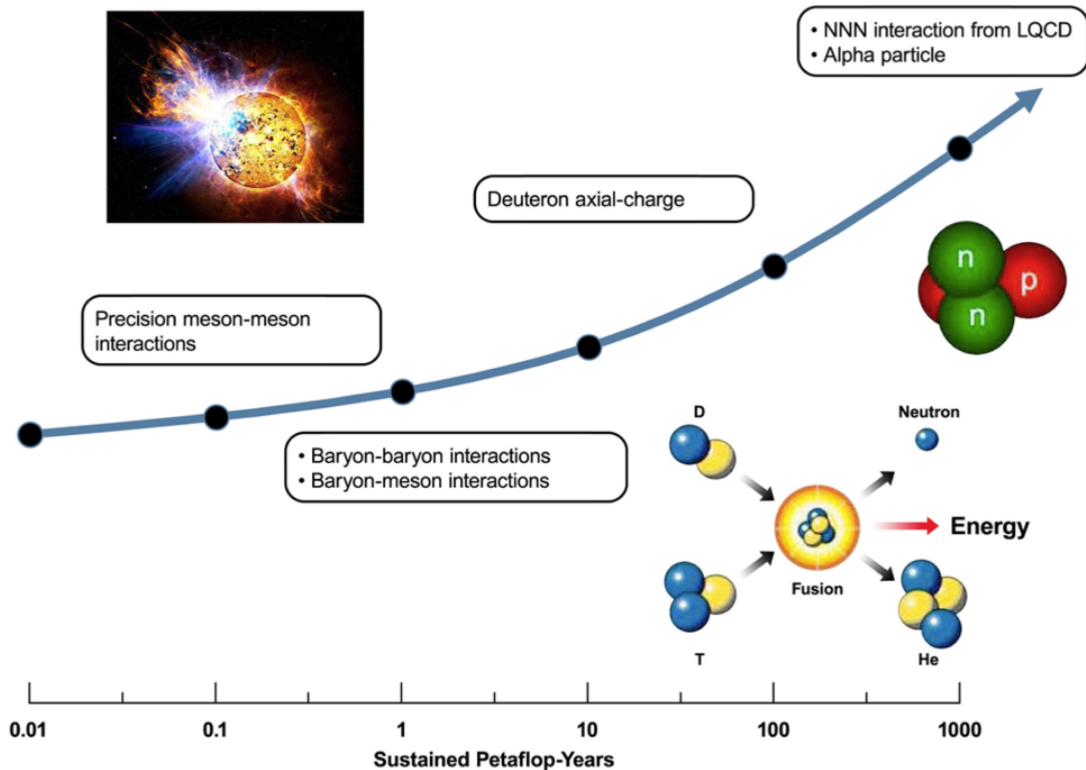


Figure 11: Estimates of the resources required to complete calculations of importance to nuclear physics [53]. Except for the quantities indicated as requiring exa-scale resources, the resource requirements are for calculations performed in the isospin limit without electroweak interactions.

Lattice QCD calculations, as indicated in Figure 11.

Despite the first Lattice QCD calculations of three- and four-baryon systems appearing recently, it is estimated that exa-scale computing resources will be required to extract precision nuclear interactions among three-nucleons and determine the spectrum of the α -particle. Given that the three-nucleon interaction is relatively imprecisely known from experiment when compared with the two-nucleon interactions, this calculation will have significant impact upon nuclear structure and reaction calculations. The three-baryon interactions between strange and non-strange baryons will be calculable with the same level of precision with minimal additional resource requirements.

Current discussions regarding exa-scale computing facilities suggest that it may be possible to see such resources deployed sometime around 2018 [53]. Clearly, such resources are required for the calculation of quantities of central importance to the nuclear physics program. During the next decade the field will develop the ability to perform low-energy strong interaction calculations with quantifiable uncertainty estimation.

5 Formal Developments

In addition to the large computational resources and algorithmic improvements that are required to complete the mission, formal developments are also required. For instance, a reliable method with which to extract inelastic scattering cross-sections from LQCD calculations does not yet exist, and must be developed. Further, a better understanding of the convergence of EFT's that are used in such systems is required. Current LQCD calculations indicate unexpected behaviors in the convergence patterns of

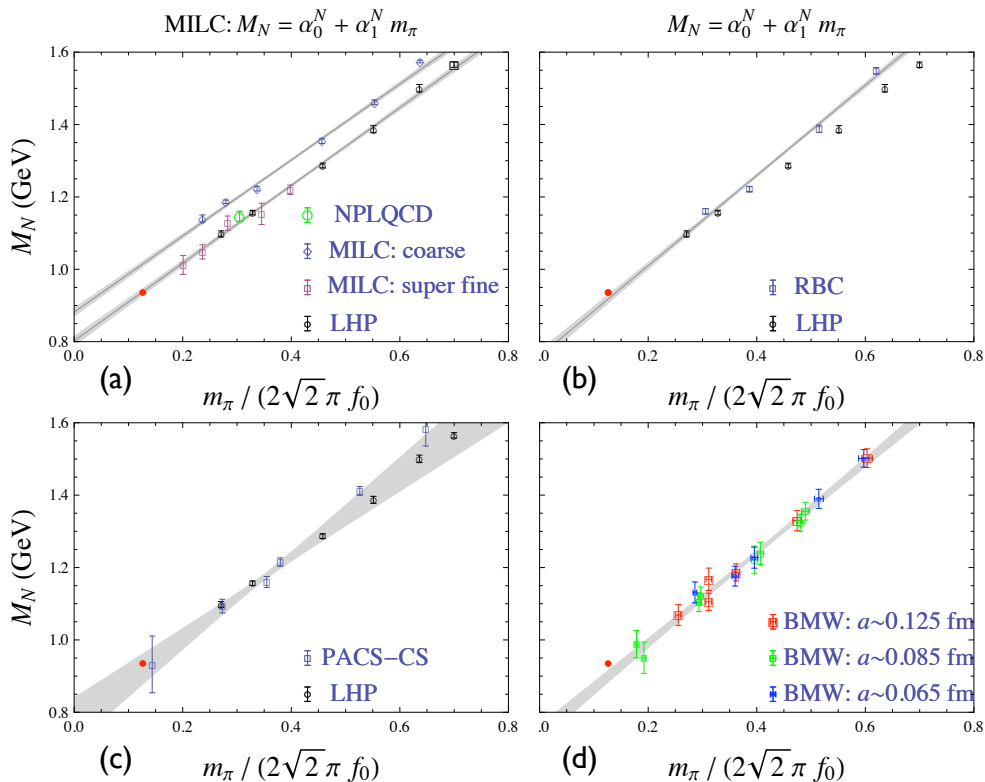


Figure 12: A summary of LQCD calculations of the mass of the nucleon (as of 2009) [60]. [Image is reproduced with the permission of A. Walker-Loud.]

the EFT's, including chiral perturbation theory (χ PT). Two striking examples of such behaviors are evident in LQCD calculations of the nucleon mass, exhibiting a light-quark mass dependence that is consistent with being linear in the pion mass (i.e. $\sqrt{m_q}$) [60], as shown in Figure 12, and in the meson-meson scattering lengths which are consistent with their tree-level predictions, even at large light-quark masses [16].

6 Outlook

A central goal of the field of nuclear physics is to establish a framework with which to perform high-precision calculations, with quantifiable uncertainties, of strong-interaction processes occurring under a broad range of conditions. Quantum chromodynamics was established as the underlying theory of the strong interactions during the 1970's, however, nuclear physics is in the regime of QCD in which its defining property of asymptotic freedom is hidden by the vacuum and by the phenomenon of confinement. Lattice QCD, in which the QCD path-integral is evaluated numerically, is the only known way to perform rigorous QCD calculations of low-energy strong interaction processes. With the research into, and development of, high-performance computing, nuclear physics, quantum-field theory, applied mathematics, and numerical algorithms that has taken place over the last few decades, the field of nuclear physics is entering into an era in which Lattice QCD will become a quantitative tool in much the same way that experiments are, but with a different scope and different range of applicability. Rapid progress is currently being made in the calculation of the interactions among the low-lying baryons. Present day Lattice QCD calculations are being performed at pion masses larger than the physical pion mass, but as exploratory calculations are now being performed at the

physical pion mass, the interactions among baryons will be known from QCD at the physical light-quark masses within the next several years (if computational resources devoted to these calculations continue to increase as they have during the last decade). These results will provide crucial input into the calculations of the structure and interactions of light nuclei. The field of nuclear physics will be somewhat revolutionized by the deployment of exa-scale computing resources as they will provide predictive capabilities that allow for the assignment of reliable uncertainty estimates in observables that cannot be explored experimentally. Further, they will enable the systematic exploration of fundamental aspects of nature that are manifested in the structure and interactions of nuclei.

I would like to thank Amand Faessler and Jochen Wambach for inviting me to participate in a most stimulating and enjoyable school. I would also like to thank all of the members of the NPLQCD collaboration for much of the progress described in this lecture.

References

- [1] C. Michael, Nucl. Phys. B **259**, 58 (1985).
- [2] M. Lüscher and U. Wolff, Nucl. Phys. B **339**, 222 (1990).
- [3] S. Syritsyn and J. W. Negele, PoS **LAT2007**, 078 (2007) [arXiv:0710.0425 [hep-lat]].
- [4] M. Lüscher, Commun. Math. Phys. **104**, 177 (1986).
- [5] L. Maiani and M. Testa, Phys. Lett. B **245**, 585 (1990).
- [6] K. Huang and C. N. Yang, Phys. Rev. **105**, 767 (1957).
- [7] M. Lüscher, Commun. Math. Phys. **105**, 153 (1986).
- [8] M. Lüscher, Nucl. Phys. B **354**, 531 (1991).
- [9] J.E. Mandula, G. Zweig and J. Govaerts, *Nucl. Phys.* **B228**, 91 (1983).
- [10] H. W. Hamber, E. Marinari, G. Parisi and C. Rebbi, Nucl. Phys. B **225**, 475 (1983).
- [11] S. R. Beane, P. F. Bedaque, A. Parreño and M. J. Savage, Phys. Lett. B **585**, 106 (2004) [arXiv:hep-lat/0312004].
- [12] S. Weinberg, Phys. Rev. Lett. **17**, 616 (1966).
- [13] G. Colangelo, J. Gasser and H. Leutwyler, Nucl. Phys. B **603**, 125 (2001) [arXiv:hep-ph/0103088].
- [14] H. Leutwyler, PoS C **CONFINEMENT8**, 068 (2008) [arXiv:0812.4165 [hep-ph]].
- [15] S. M. Roy, Phys. Lett. B **36**, 353 (1971).
- [16] S. R. Beane, T. C. Luu, K. Orginos, A. Parreno, M. J. Savage, A. Torok and A. Walker-Loud, Phys. Rev. D **77**, 014505 (2008) [arXiv:0706.3026 [hep-lat]].
- [17] X. Feng, K. Jansen and D. B. Renner, Phys. Lett. B **684**, 268 (2010) [arXiv:0909.3255 [hep-lat]].
- [18] T. Yamazaki *et al.* [CP-PACS Collaboration], Phys. Rev. D **70**, 074513 (2004) [arXiv:hep-lat/0402025].
- [19] J. J. Dudek, R. G. Edwards, M. J. Peardon, D. G. Richards and C. E. Thomas, Phys. Rev. D **83**, 071504 (2011) [arXiv:1011.6352 [hep-ph]].
- [20] S. R. Beane *et al.* [NPLQCD Collaboration], arXiv:1107.5023 [hep-lat].
- [21] R. L. Jaffe, Phys. Rev. Lett. **38**, 195 (1977); **38**, 617 (1977)(E).
- [22] V. G. J. Stoks and T. A. Rijken, Phys. Rev. C **59**, 3009 (1999) [arXiv:nucl-th/9901028].
- [23] G. A. Miller, arXiv:nucl-th/0607006.
- [24] J. Haidenbauer, U. -G. Meissner, Phys. Lett. **B684**, 275-280 (2010). [arXiv:0907.1395 [nucl-th]].

- [25] S. R. Beane *et al.* [NPLQCD Collaboration], Phys. Rev. Lett. **106**, 162001 (2011) [arXiv:1012.3812 [hep-lat]].
- [26] S. R. Beane *et al.* [NPLQCD Collaboration], arXiv:1109.2889 [hep-lat].
- [27] T. Inoue *et al.* [HAL QCD Collaboration], Phys. Rev. Lett. **106**, 162002 (2011) [arXiv:1012.5928 [hep-lat]].
- [28] S. R. Beane *et al.*, arXiv:1103.2821 [hep-lat].
- [29] P. E. Shanahan, A. W. Thomas and R. D. Young, arXiv:1106.2851 [nucl-th].
- [30] J. Haidenbauer and U. G. Meissner, arXiv:1109.3590 [hep-ph].
- [31] http://j-parc.jp/NuclPart/index_e.html
- [32] J. Steinheimer, M. Mitrovski, T. Schuster, H. Petersen, M. Bleicher and H. Stoecker, Phys. Lett. B **676**, 126 (2009) [arXiv:0811.4077 [hep-ph]].
- [33] http://j-parc.jp/NuclPart/pac_1107/pdf/KEK_J-PARC-PAC2011-03.pdf
- [34] T. Yamazaki, Y. Kuramashi, A. Ukawa, arXiv:1105.1418 [hep-lat].
- [35] T. Yamazaki, Y. Kuramashi, A. Ukawa, Phys. Rev. D **81**, 111504 (2010) [arXiv:0912.1383 [hep-lat]].
- [36] D. B. Kaplan, M. J. Savage, M. B. Wise, Phys. Lett. **B424**, 390-396 (1998). [nucl-th/9801034].
- [37] M. C. Birse, J. A. McGovern, K. G. Richardson, Phys. Lett. **B464**, 169-176 (1999). [hep-ph/9807302].
- [38] S. R. Beane and M. J. Savage, Nucl. Phys. A **713**, 148 (2003) [arXiv:hep-ph/0206113].
- [39] S. R. Beane and M. J. Savage, Nucl. Phys. A **717**, 91 (2003) [arXiv:nucl-th/0208021].
- [40] E. Epelbaum, U. G. Meissner and W. Gloeckle, Nucl. Phys. A **714**, 535 (2003) [arXiv:nucl-th/0207089].
- [41] M. Fukugita, Y. Kuramashi, H. Mino, M. Okawa and A. Ukawa, Phys. Rev. Lett. **73**, 2176 (1994) [arXiv:hep-lat/9407012].
- [42] M. Fukugita, Y. Kuramashi, M. Okawa, H. Mino and A. Ukawa, Phys. Rev. D **52**, 3003 (1995) [arXiv:hep-lat/9501024].
- [43] S. R. Beane, P. F. Bedaque, K. Orginos and M. J. Savage, Phys. Rev. Lett. **97**, 012001 (2006) [arXiv:hep-lat/0602010].
- [44] S. R. Beane, P. F. Bedaque, T. C. Luu, K. Orginos, E. Pallante, A. Parreno and M. J. Savage [NPLQCD Collaboration], Nucl. Phys. A **794**, 62 (2007) [arXiv:hep-lat/0612026].
- [45] S. R. Beane *et al.* [NPLQCD Collaboration], Phys. Rev. D **81**, 054505 (2010) [arXiv:0912.4243 [hep-lat]].
- [46] S. Aoki, T. Hatsuda and N. Ishii, Comput. Sci. Dis. **1**, 015009 (2008) [arXiv:0805.2462 [hep-ph]].
- [47] S. Aoki, T. Hatsuda and N. Ishii, Prog. Theor. Phys. **123**, 89 (2010) [arXiv:0909.5585 [hep-lat]].
- [48] N. Ishii, S. Aoki and T. Hatsuda, Phys. Rev. Lett. **99**, 022001 (2007) [arXiv:nucl-th/0611096].
- [49] D. T. Son and M. A. Stephanov, Phys. Rev. Lett. **86**, 592 (2001) [arXiv:hep-ph/0005225].
- [50] W. Detmold, K. Orginos, M. J. Savage and A. Walker-Loud, Phys. Rev. D **78**, 054514 (2008) [arXiv:0807.1856 [hep-lat]].
- [51] D. B. Kaplan and A. E. Nelson, preprint HUTP-86/A023; Phys. Lett. B **175** (1986) 57; Phys. Lett. B **192**, 193 (1987); Nucl. Phys. A **479**, 273 (1988); Nucl. Phys. A **479**, 285 (1988);
- [52] W. Detmold and B. Smigielski, Phys. Rev. D **84**, 014508 (2011) [arXiv:1103.4362 [hep-lat]].
- [53] Scientific Grand Challenges: Forefront Questions in Nuclear Science and the Role of Computing at the Extreme Scale. A workshop sponsored by the Office of Nuclear Physics and the Office of Advanced Scientific Computing Research, held in January 2009. The report is available from <http://extremecomputing.labworks.org/nuclearphysics/report.stm>

- [54] M. J. Savage, AIP Conf. Proc. **1343**, 30 (2011) [arXiv:1012.0876 [nucl-th]].
- [55] S. R. Beane, K. Orginos and M. J. Savage, Int. J. Mod. Phys. E **17**, 1157 (2008) [arXiv:0805.4629 [hep-lat]].
- [56] S. R. Beane, W. Detmold, K. Orginos and M. J. Savage, Prog. Part. Nucl. Phys. **66**, 1 (2011) [arXiv:1004.2935 [hep-lat]].
- [57] A. A. Khan *et al.*, Phys. Rev. D **74**, 094508 (2006) [arXiv:hep-lat/0603028].
- [58] J. D. Bratt *et al.* [LHPC Collaboration], arXiv:1001.3620 [hep-lat].
- [59] T. Yamazaki *et al.*, Phys. Rev. D **79**, 114505 (2009) [arXiv:0904.2039 [hep-lat]].
- [60] A. Walker-Loud, PoS **LATTICE2008**, 005 (2008) [arXiv:0810.0663 [hep-lat]].